# Damping and dispersion of linear longitudinal oscillations in a multi-component plasma. II

Physica 85C (1977) 357–364


# DAMPING AND DISPERSION OF LINEAR LONGITUDINAL OSCILLATIONS IN A MULTI-COMPONENT PLASMA. II

A. J. D. LAMBERT, F. W. SLUIJTER and D. C. SCHRAM
*Department of Applied Physics, Technische Hogeschool Eindhoven, The Netherlands*

Received 22 November 1976

Linear dispersion-phenomena in Vlasov–Poisson plasma's with drift are studied in order to be able to test the relevance of linear theory for plasma turbulence. Especially the effect of the addition of light ions, giving rise to stabilisation, is taken into account. Emphasis is laid on approximate methods that give the possibility to investigate the influence of parameters like ion-mass-ratio, temperature ratio etc. Numerical results are given for a He-A plasma.

## 1. Introduction

In a previous article [1] (indicated as I) we discussed the dispersion of longitudinal waves in a plasma, using a linearised Vlasov–Poisson system. It was our aim to give the necessary background for using the presence of more than one ion species as a means to test the relevance of linear concepts in the early stages of the development of turbulence. In this article we extend the previous treatment to include the presence of electron drift.

First, we study the one ion species plasma and look especially at the influence of the electron-ion temperature ratio on the topology of the critical electron drift vs. phase velocity curve. The case of the electrons hotter than the ions is investigated rigorously. The dependence of some characteristic points of that curve on the temperature ratio and on the ion mass is determined. Then we investigate the modifications of this theory upon addition of another ion species.

Consequently two new parameters arise: the ion mass ratio and the light ion fraction. Finally we make some numerical calculations for a He-A plasma with an electron-ion-temperature ratio of 50. At least for this case the approximate methods we develop prove to be rather accurate.

## 2. Basic concepts

Starting again from Maxwellian distributions we obtain the same dispersion relation as in (I.9). However, the electrons now possess an average drift velocity $v_d$, which can be normalised in the same way as before with the help of the thermal speed $v_e$ according to

$$u = v_d/(v_e\sqrt{2}). \tag{1}$$

Then the argument $\xi_e$ reads:

$$\xi_e = -u + (\tilde{\omega}_1 + i\tilde{\gamma}_1)(\theta\delta)^{-\frac{1}{2}} = \tilde{\omega}_e + i\tilde{\gamma}_e. \tag{2}$$

As long as $|\tilde{\gamma}| \ll |\tilde{\omega}|$ the approximate expressions:

$$2k^2 = \mathrm{Re}\, Z'(-u + \tilde{\omega}_1(\theta\delta)^{-\frac{1}{2}}) + \theta\ \mathrm{Re}\, Z'(\tilde{\omega}_1) \tag{3}$$

and

$$\tilde{\gamma} = (4\pi/\delta)^{\frac{1}{2}} \times \left\{ \frac{[-u + \tilde{\omega}_1(\theta\delta)^{-\frac{1}{2}}]\ e^{-[u - \tilde{\omega}_1(\theta\delta)^{-\frac{1}{2}}]^2} + \theta\tilde{\omega}_1 e^{-\tilde{\omega}_1^2}}{\dfrac{\mathrm{d}\ \mathrm{Re}\, Z'(\tilde{\omega}_e)}{\mathrm{d}\,\tilde{\omega}_e} + (\theta^3\delta)^{\frac{1}{2}} \dfrac{\mathrm{d}\ \mathrm{Re}\, Z'(\tilde{\omega}_1)}{\mathrm{d}\,\tilde{\omega}_1}} \right\} \tag{4}$$

are valid.

An essential extension with respect to the case treated in I is the possibility of solutions with $\tilde{\gamma} > 0$, i.e. instable solutions. Physically relevant and rather simple is an analysis of the case $\tilde{\gamma} = 0$, i.e. the marginally stable solution. In general there are two different marginally stable solutions of $u$ for every $\tilde{\omega}$; that value of $u$ which is closest to zero, is called the critical drift.

We will mainly concentrate on the case $\theta > 1$, and consider the plasma with only one ion species first; subsequently the two-ion species plasma will be our concern.

In the $\tilde{\gamma} = 0$-case only the denominator of (4) is of interest. If it is zero we obtain what we will call the basic equation:

$$[-u + \tilde{\omega}_1(\theta\delta)^{-\frac{1}{2}}]\, e^{-[u - \tilde{\omega}_1(\theta\delta)^{-\frac{1}{2}}]^2} + \theta\tilde{\omega}_1\, e^{-\tilde{\omega}_1^2} = 0. \quad (5)$$

We will give a plot of $u$ vs. $\tilde{\omega}_1$ for marginally stable solutions.

## 3. Qualitative analysis of marginally stable solutions

Fig. 1 gives a plot of $u$ vs. $\tilde{\omega}_1$ for $\theta > 1$. Its physical content is related to fig. 1 of I. The plot can easily be understood with the help of Jackson's graphical method [2]. The method is demonstrated in fig. 5. The method is based on the full dispersion relation (I.9):

$$2k^2/\theta = Z'(\xi_e)/\theta + Z'(\xi_1). \quad (6)$$

Fig. 5 shows (in the case $\tilde{\gamma} = 0$) how the value

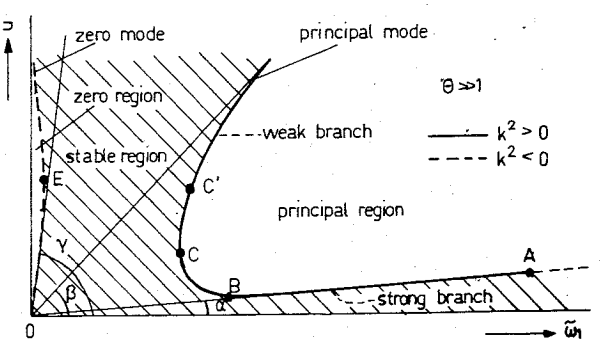


Fig. 1. $u$ vs. $\tilde{\omega}_1$-plot of stable and instable regions and marginal instability for a single-component plasma at $\theta \gg 1$.

$2k^2/\theta$ is constructed from the $Z'(\xi_1)$ and $Z'(\xi_e)$ plots in the complex $Z'$-plane, where $\tilde{\omega}_1$ and $-u + \tilde{\omega}_1(\theta\delta)^{-\frac{1}{2}}$ are the parameters. With this method we obtain values of $u$ and $\tilde{\omega}_1$ for the cutoff (in fig. 1 indicated by A) where $k^2 = 0$ (fig. 5c). To the right of A, the marginally stable solutions are evanescent ($k^2 < 0$), indicated in fig. 1 by a dashed line. Points C′ and E′ in fig. 1 are points with a maximum value of $k^2$ (cf. figs. 5a and 5d, respectively). Point C is the point of the principal mode with minimum $\tilde{\omega}_1$; point E is that of the zero mode with maximum $\tilde{\omega}_1$. (cf. figs. 5b resp. 5e.) The plot of fig. 1 can be found straightforwardly from the basic equation (5).

To that end we have to compare the slopes of the two (reduced) distribution functions plotted in one figure. The slope of the ion distribution function has to be inverted, that of the electron distribution function has to be shifted over a distance $u\sqrt{\theta\delta}$ along the positive $\tilde{\omega}_1$-axis (fig. 4). If it is shifted to the right ($u > 0$), there are in general three intersection points (Z, W and S) all within the interval $0 < \tilde{\omega}_1 < u/\sqrt{\theta\delta}$, i.e. the interval in which the slopes of the ion- and electron-distribution functions have opposite signs. Z, W and S represent points of respectively the zero mode, the weak and strong branch of the principal mode, as indicated in fig. 1.

As will be shown, for relatively high $\theta$-values ($\theta \gtrsim 25$), point A is well separated from point B and to the right of it (point B represents the minimal critical drift). Then there exists a $u$-interval where to every $u$ there are two physically relevant marginally stable $\tilde{\omega}_1$-values: one to the left of point B, and one in the interval between A and B. At the latter $\tilde{\omega}_1$-value, corresponding to point S in fig. 4, the slope of the electron distribution function is small and positive, but there are many electrons there. The slope of the ion distribution function is negative but there are only a few of them with the required velocity. The combined effect is of course just zero: electron Landau instability is exactly compensated by ion Landau damping. On the other hand at a smaller $\tilde{\omega}_1$ the slope of the electron distribution function increases, but there is again a point where the ions due to their (increased negative) slope are again able to balance the (electron) Landau instability (point W). For phase velocities between these two points the slope and value of the ion distribution is unable to stabilise the electron instability.

In fact there is always a third $\tilde{\omega}_1$ belonging to a certain $u$. This is due to the circumstance that at $u = 0$ there is also formally a compensation, because both ion and electron distribution slopes are equal to zero as the two Gaussians have the same central line. A certain separation of the central lines leads to a small but finite $u$ (point Z) for this compensation. One can also look at it from another point of view. Between W and Z the ion damping is dominant. Although the number of ions with small velocities increases, the slope of the distribution approaches zero as one approaches the phase velocity 0. To the left of Z therefore the electrons win again and we have dominance of the electron Landau instability. However, when $\theta > 1$, the electron distribution slope cannot become sufficiently large to overcome the ion Landau damping for values of $\tilde{\omega}_1$ to the right of the rightmost point E (see fig. 1). Point B can be found from fig. 4 by shifting the curve of the electron slope to the left, until W and S coincide. This is represented by the dotted curve.

If $\theta = 1$ the balancing of electron instability and ion Landau damping goes right through and point E coincides with the leftmost point (point C) of the principal mode (fig. 2). This is easily understood by using Jackson's method; cf. fig. 5 and take $\theta = 1$.

If $\theta < 1$ the branches break up again due to overcompensation of the ion Landau damping by the electron instability. The weak branch of the principal mode will be connected to the upper part of the zero mode, to form the high drift branch. In the same way the strong branch will transform continuously into the lower part of the zero mode to form the low drift mode (fig. 3).

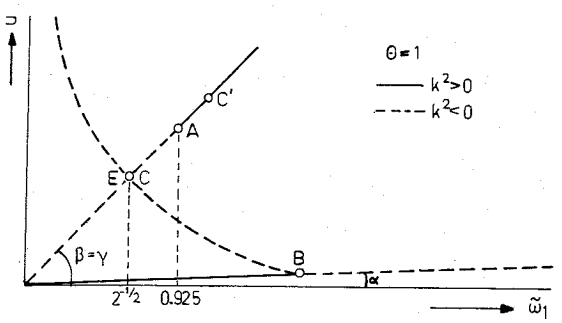


Fig. 2. Stable and instable regions for a single-component plasma at $\theta = 1$.

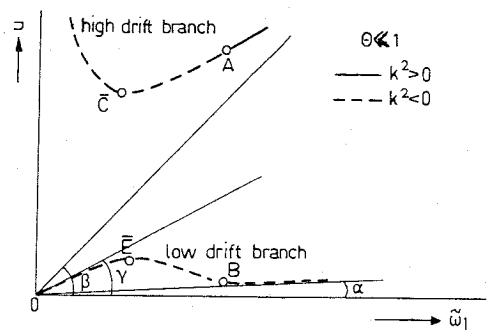


Fig. 3. Stable and instable regions for a single-component plasma at $\theta \ll 1$.

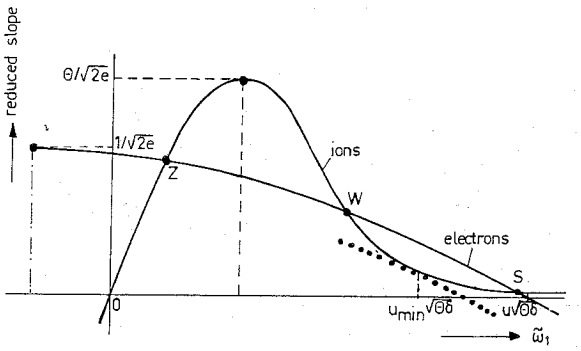


Fig. 4. Determination of $\tilde{\omega}_1$-values at fixed $u$ from the reduced slopes of the distribution functions, that occur as terms in the basic equation.

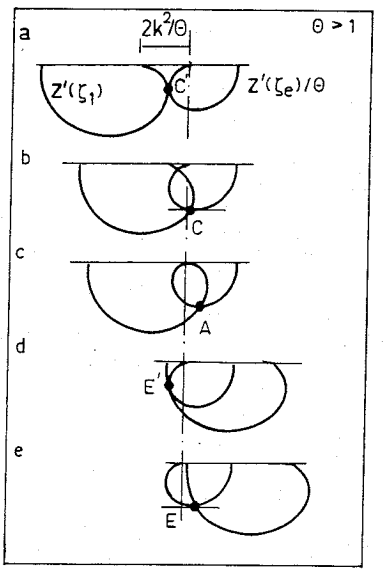


Fig. 5. Jackson's method for the evaluation of different characteristic points of the marginal stability plot of fig. 1.

## 4. Quantitative analysis

First we will consider the strong branch ($\theta > 1$). As we are not concerned with an electron-hole plasma (which would mean $\delta$ rather close to unity) it is not difficult to assure a sufficiently large $\theta$ such that

$$|-u + \tilde{\omega}_1(\theta\delta)^{-\frac{1}{2}}| \ll 1; \tag{7}$$

and then (5) reduces to

$$u = \theta\tilde{\omega}_1\{(\theta^3\delta)^{-\frac{1}{2}} + e^{-\tilde{\omega}_1^2}\}. \tag{8}$$

For rather large $\tilde{\omega}_1$ values the exponential may be neglected and the relation between $u$ and $\tilde{\omega}_1$ becomes a linear one. This leads to an asymptote for the strong branch, the angle $\alpha$ given by

$$\alpha = \arctan(\theta\delta)^{-\frac{1}{2}}. \tag{9}$$

The weak branch also has an asymptote that can be found from (5). One finds

$$\beta = \arctan(1 + (\theta\delta)^{-\frac{1}{2}}), \tag{10}$$

i.e. almost $\pi/4$. Hence the weak branch approaches approximately $\tilde{\omega}_1 = u$.

The zero branch represents the drift modified version of the trivial solution of (3) with $u = 0$, viz. $\tilde{\omega}_1 = 0$, $\tilde{\gamma}$ arbitrary; $k^2 < 0$. We can find the angle $\gamma$ from (8) by calculating $du/d\tilde{\omega}_1$ in the limit $\tilde{\omega}_1 \to 0$:

$$\gamma = \arctan(\theta + (\theta\delta)^{-\frac{1}{2}}). \tag{11}$$

In the first place this is proof of the fact that our picture of balancing Landau damping and Landau instability due to ions and electrons respectively is correct. One should further note that in the limit of $\theta \to 1$, $\gamma \to \beta$ (cf. fig. 2).

We now proceed with the determination of the characteristic points in fig. 1.

*Point A*, the cutoff, is easily determined. It can be found from (3), taking into account condition (7) that is valid for $\theta \gtrsim 25$. Then the equation for point A reduces to

$$2 \cong \theta \operatorname{Re} Z'(\tilde{\omega}_1). \tag{12}$$

Replacing the right-hand side by its asymptotic expression leads to

$$\tilde{\omega}_1 \cong \sqrt{\theta/2}, \tag{13}$$

provided $\theta \gtrsim 30$.

*Point B*, the minimum of the principal mode, is found from (8), leading to

$$(2\tilde{\omega}_1^2 - 1)\, e^{-\tilde{\omega}^2} = (\theta^3\delta)^{-\frac{1}{2}}. \tag{14}$$

For several values of $\delta$ the relation between $\tilde{\omega}_1$ and $\theta$ has been plotted (fig. 6). In the physically relevant region (i.e. $1 \lesssim \theta \lesssim 100$) the $\tilde{\omega}_1$ belonging to point B does not vary very much. Its value is close to 3 throughout this domain. With decreasing $\theta$, $\tilde{\omega}_1$ at point B decreases much slower than $\tilde{\omega}_1$ at point A. This means that points A and B approach each other until they coincide at some critical $\theta$-value which appears to be approximately 25, and which is weakly $\delta$-dependent. A plot of the critical $\theta$-value vs. $\delta$ is given in fig. 7.

Fig. 8 of [3], a plot that shows the critical drift vs. $\theta$, is closely connected with this consideration (there

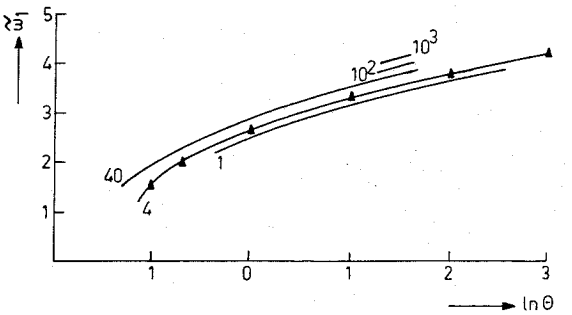


Fig. 6. $\theta$-dependence of the $\tilde{\omega}_1$-value at point B.

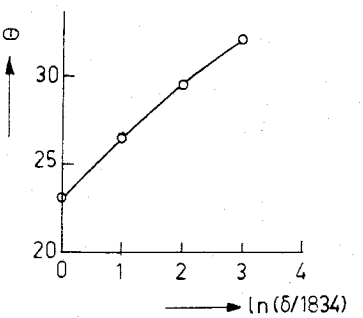


Fig. 7. $\delta$-dependence of the critical $\theta$-value (A and B coincide).

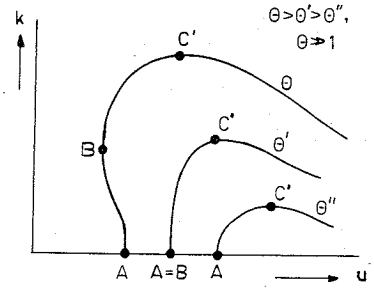


Fig. 8. $k$ vs. $u$ plot and its relation to the characteristic points.

$\theta_{krit} \approx 20$). Fig. 7 should not be trusted too much, because of the approximations made, but it is sufficiently accurate for a global discussion. In $k$ vs. $u$ plots, as given in [2] and [4], $\theta \approx 25$ is the curve that starts vertically from the $u$-axis and marginally does not bend towards the $k$-axis anymore ($d^2u/dk^2|_{k=0} = 0$) (fig. 8).

These plots also give a clear meaning to *point C'*. It corresponds to the maximum $k$-value where instability may occur. Its occurrence is most easily understood from fig. 5a; the electron and ion loci have only one point in common. This means that there is a unique correspondence between $k$, $u$ and $\tilde{\omega}_1$. The $\theta$-dependence of these values is plotted in fig. 9. The *point E'* is the counterpart of C' on the zero mode (fig. 5d).
*Point C* can be found by considering the situation where $u$ is such that the electron branch is intersected by the ion branch exactly at the point where Im $Z'(\xi_e)$ has its extremum, that is at $\tilde{\omega}_e = -1/\sqrt{2}$, where Im $Z'(\xi_e) = (2e)^{-\frac{1}{2}}$.

With the help of (5) one finds the following

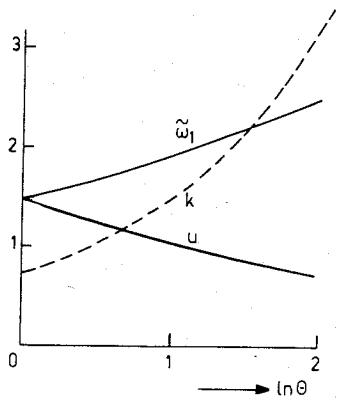


Fig. 9. $\theta$-dependence of the $\tilde{\omega}_1$, $k$ and $u$-values, belonging to point C'.

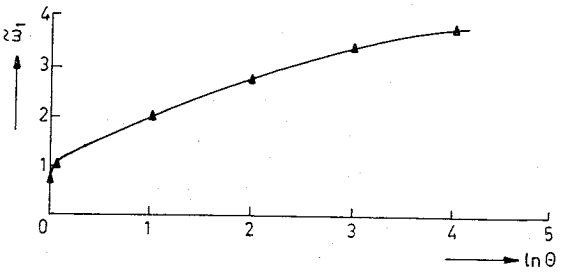


Fig. 10. $\theta$-dependence of the $\tilde{\omega}_1$-value at point C.

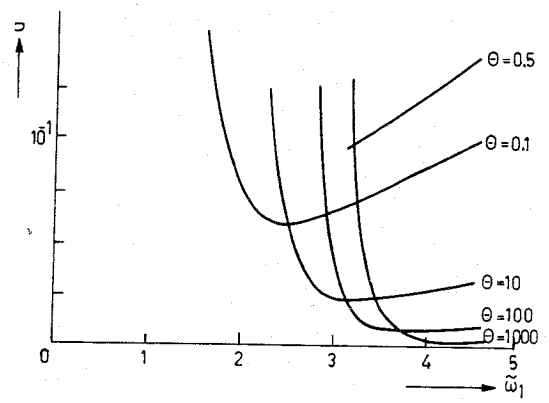


Fig. 11. Exact $u$ vs. $\tilde{\omega}_1$-plots for a proton plasma at a wide range of $\theta$-values (computer calculation).

expression for $\tilde{\omega}_1$ at C:

$$\tilde{\omega}_1 \exp(-\tilde{\omega}_1^2) = (\theta\sqrt{2e})^{-1} \tag{15}$$

by taking that branch of the solution for which $\tilde{\omega}_1 > 1/\sqrt{2}$. As is clear from fig. 10, $\tilde{\omega}_1$ at point C is only a weak function of $\theta$ for the physically relevant $\theta$-range. $\tilde{\omega}_1$ at point C is approximately 2. The critical drift velocity at C is practically $1/\sqrt{2}$, because for $\tilde{\omega}_1 \approx 2$,

$$\xi_e = -u + \tilde{\omega}_1(\theta\delta)^{-\frac{1}{2}} \approx -u = -\tfrac{1}{2}\sqrt{2}. \tag{16}$$

With the aid of a digital computer we computed in the case of a proton plasma ($\delta \approx 1834$) a $u$ vs. $\tilde{\omega}_1$-plot at different $\theta$-values (fig. 11).

## 5. Stabilisation by light ions

We will now consider the influence of a small fraction of light ions. We can restrict ourselves to this case only without any loss of generality. The parameter

range that would mean addition of heavy ions to a light ion plasma is not very interesting. The distribution function of heavy ions of the same temperature as that of light ions has a smaller width than that of the latter. Only the introduction of a species that has a distribution function with a width in between those of the dominant ion species and electrons gives rise to interesting phenomena. In order to be able to find quantitative results that can be derived at easily with analytical means, we restrict ourselves to the case $\theta \gg 1$. Moreover, we know that for $\theta$ closer to 1 the situation is intrinsically rather stable, because the critical drift at B increases (fig. 11) and, for $\theta \lesssim 25$, A is on the weak branch to the left of B (e.g. see fig. 2). So the detailed Landau instability damping balance is not very interesting anymore.

In the case $\tilde{\gamma} = 0$, the basic equation (5) is modified for the presence of the second ion species and reads:

$$[-u + \tilde{\omega}_1(\theta\delta)^{-\frac{1}{2}}]\, e^{-[u - \tilde{\omega}_1(\theta\delta)^{-\frac{1}{2}}]^2} + \theta\eta\tilde{\omega}_1 e^{-\tilde{\omega}_1^2} + \theta(1-\eta)\mu^{\frac{1}{2}}\tilde{\omega}_1 e^{-\mu\tilde{\omega}_1^2} = 0. \quad (17)$$

The real part of the dispersion relation gives:

$$2k^2 = \mathrm{Re}\, Z'(-u + \tilde{\omega}_1(\theta\delta)^{-\frac{1}{2}}) + \theta\eta\, \mathrm{Re}\, Z'(\tilde{\omega}_1) + \theta(1-\eta)\, \mathrm{Re}\, Z'(\tilde{\omega}_1\mu^{\frac{1}{2}}), \quad (18)$$

where $\eta$ is again the fraction of the light ions over the total number, while $\mu$ represents the mass ratio of the heavy ions over the light ones.

We will now discuss the changes of the characteristic points of fig. 1 and first of all we retrace the counterpart of *point A*. We will use the subscript 1 because of the convention that we normalise all quantities with respect to light-ion ones. If $\tilde{\omega}_1 \gtrsim 4$ and $|u - \tilde{\omega}_1(\theta\delta)^{\frac{1}{2}}| \ll 1$ the asymptotic expansions of $Z'$ may be used for both ion terms in equation (18) while the electron term reduces to $-2$. Then we can introduce, (cf. I):

$$M = \eta + \frac{1-\eta}{\mu} \quad (19)$$

and eq. (18) gives us for the value of $\tilde{\omega}_1$, belonging to $k^2 = 0$:

$$\tilde{\omega}_1 \cong \sqrt{\theta M/2}. \quad (20)$$

The introduction of the light ions forces $M$ to grow gradually from $\mu^{-1}$ to 1. Consequently point A moves gradually from $\tilde{\omega}_1 = \sqrt{\theta/2\mu}$ to $\tilde{\omega}_1 = \sqrt{\theta/2}$. This change is in fact trivial because of the normalisation.

The minimal critical drift, corresponding to *point B* in fig. 1, can be calculated with the aid of (17). In the case $\mu$ not too small, the exponential will, in general, make the heavy-ion contribution small. Close to B we have

$$|u - \tilde{\omega}_1(\theta\delta)^{-\frac{1}{2}}| \ll 1 \quad (21)$$

and, if the rather mild condition on $\tilde{\omega}_1$

$$\eta\, e^{-\tilde{\omega}_1^2} \gg (1-\eta)\sqrt{u}\, e^{-\mu\tilde{\omega}_1^2} \quad (22)$$

holds, it is permitted to neglect the heavy-ion term at all. Then we obtain from (17):

$$(2\tilde{\omega}_1^2 - 1)\, e^{-\tilde{\omega}_1^2} = (\delta^{\frac{1}{2}}\theta^{\frac{3}{2}}\eta)^{-1}; \quad (23)$$

this is the same expression as (14), when we substitute:

$$\theta' = \theta\eta^{\frac{2}{3}}. \quad (24)$$

With the aid of fig. 6 we obtain an $\tilde{\omega}_1$-value, after the calculation (21) and (22) have to be checked; for a sufficiently small $\eta$ (22) may not be satisfied.

To conclude this section, we want to consider the part of the principal mode that starts from point B in the direction of diminishing $\tilde{\omega}_1$. Then (21) is certainly not satisfied. If, however,

$$\tilde{\omega}_1(\theta\delta)^{-\frac{1}{2}} \ll 1 \quad (25)$$

the electron contribution can be approximated by $-u\, e^{-u^2}$. If subsequently (22) is satisfied, the basic equation reduces to

$$-u\, e^{-u^2} + \theta\eta\tilde{\omega}_1 e^{-\tilde{\omega}_1^2} = 0 \quad (26)$$

and if we substitute $u = 1/\sqrt{2}$, as in (16), we obtain the same expression for $\tilde{\omega}_1$ at C, but we have to replace $\theta$ by $\theta''$, given by

$$\theta'' = \theta\eta. \quad (27)$$

We find an $\tilde{\omega}_1$-value with the help of fig. 10. If, how-

ever $\theta'' \lesssim 1$, there is practically no change in the $\tilde{\omega}_1$-value at C, compared with that of the pure heavy-ion plasma, while it is quite possible that $\tilde{\omega}_1$ at B has changed considerably. Of course (22) and (25) need to be checked.

We may conclude that for a large $\theta$ (e.g. between 10 and as large as 200) the appearance of a trace of light ions has a pronounced effect on the minimal critical drift due to the large difference in broadness of the distribution function of the light ions in comparison with that of heavy ions of the same temperature. Below $\theta \approx 10$ and above $\theta \approx 200$ (if one would be able to reach such a $\theta$), the effect becomes rapidly less pronounced and will disappear. If $\theta$ is sufficiently large, B will stay to the left of A. For $\theta$ sufficiently low A will always be to the left of B. Strong stabilisation is the result, or in other words, the minimal critical drift becomes large (in absolute value). If $\eta$ proceeds towards 1, B does not shift very much to the right anymore, but now A shifts considerably and will again end up to the right of B. The instability will again set in at small $u$.

The whole discussion is based on one ion temperature. It will be clear from the dependence of the effect on the detailed form of the distribution function of the light ions, that a higher temperature of the light ions would further enhance the critical drift.

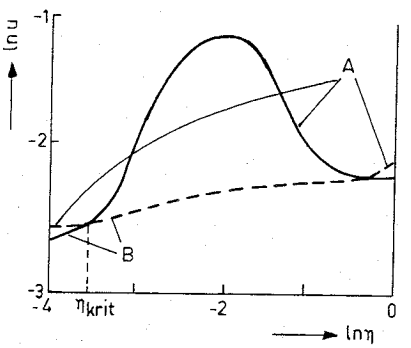


Fig. 12. Schematic plot of the $u$-values belonging to A and B vs. ln $\eta$ and its relation to the actual physically relevant minimal critical drift.

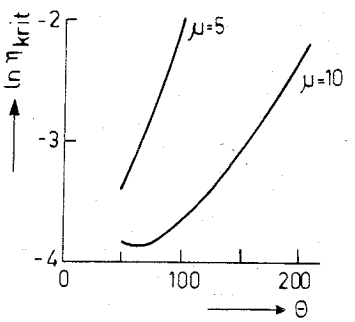


Fig. 13. The influence of $\theta$ and $\mu$ on the minimal $\eta$-value required for stabilisation.

## 6. Some calculations

As an illustration as well as a verification we have executed two types of calculations, one, analytically with the aid of approximate formulae as described above, the other starting from the exact dispersion relation with the aid of a digital computer. We are able to extend the latter calculations to cases with (either positive or negative) damping. Calculations are made for a He-A plasma with $\theta = 50$: a value where stabilisation effects are pronounced.

At very low $\eta$-values point A hardly changes its position, but B goes rapidly to the right. At a critical value of $\eta$, B overtakes A (fig. 12) and the minimal critical drift is at point A instead of at point B. The value of the minimal critical drift, with increasing $\eta$ goes through a maximum value, and then decreases again. At an $\eta$-value of, e.g., 5, A overtakes B again and the minimal critical drift, at B, is small again.

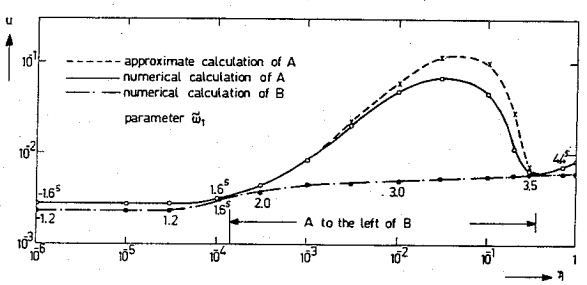


Fig. 14. Approximate calculation of $u$ at A, compared with a numerical calculation of $u$ at A and B, for a He-A plasma at $\theta = 50$. Parameter $\tilde{\omega}_1$.

Fig. 13 shows the $\theta$-dependence of the critical $\eta$-value and its strong $\mu$-dependence is illustrated. The dashed line in fig. 14 shows the results of the approximate calculation. The continuous line shows the result of the exact calculation and it is easily seen that at low $\eta$-values the approximation is very useful and leads to

good estimations of the contamination damping.

At the region of very high $u$-values the approximation is no longer valid because of the fact that (21) no longer holds. To the right of the top there is a discrepancy because it is not possible to determine point A accurately enough with analytical means because $\tilde{\omega}_1 < 4$ and the light-ion term in the full dispersion relation cannot be neglected anymore: the $\eta$-value is then rather large. When $\tilde{\omega}_1 \gtrsim 4$ at $\eta$-values in the neighbourhood of 1, the approximate results are again in accordance with the exact results. Fig. 15 gives some $u$ vs. $\tilde{\omega}_1$-plots of a helium–argon plasma at different $\eta$-values. These plots are parametrised with $k^2$. Fig. 16 gives a blow-up of the strong branch, showing the movement of A and B at different $\eta$-values.

We close this section with two calculations for the damped cases $\tilde{\gamma} = \pm 0.05$ and we see the influence of $\tilde{\gamma}$ on the $u$ vs. $\tilde{\omega}_1$-plots for a helium plasma (fig. 17). Fig. 18 is again a blow-up. Of course an intersection with the real $\tilde{\omega}_1$ axis has to be expected, because there exists a damped mode when there is no drift at all.

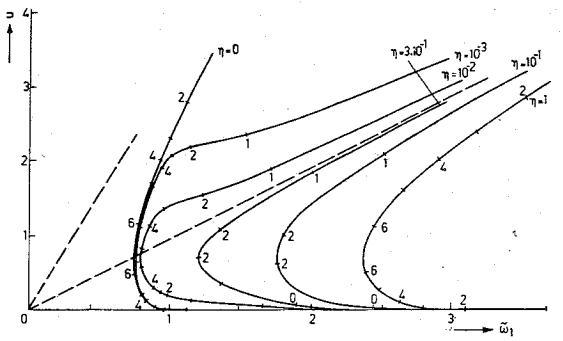


Fig. 15. Numerical calculations of a $u$ vs. $\tilde{\omega}_1$-plot at different $\eta$-values for a He-A plasma at $\theta = 50$. $k^2$ is a parameter along the curves.

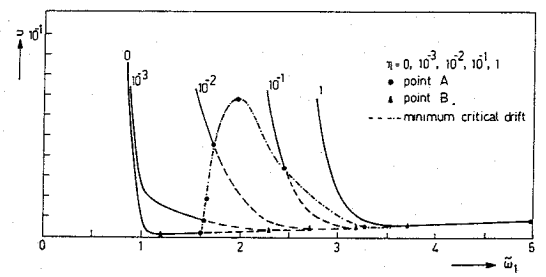


Fig. 16. Blow-up of the plot of fig. 15, near the $\tilde{\omega}_1$-axis.

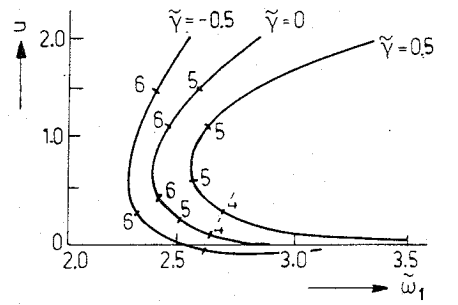


Fig. 17. $u$ vs. $\tilde{\omega}_1$-plot of a He-plasma at different values of $\tilde{\gamma}_1$ (numerical).

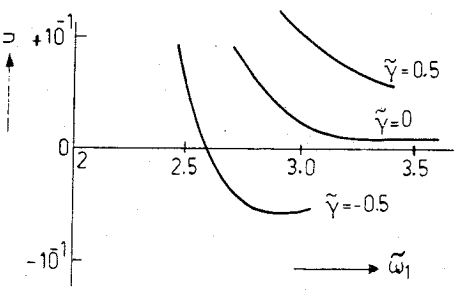


Fig. 18. Blow-up of the plot of fig. 17, near the $\tilde{\omega}_1$-axis.

## 7. Conclusion

In conclusion we observe that, provided one is in the appropriate temperature ratio interval, the addition of a small fraction of light ions has a profound stabilising effect. Thus this effect may be used to suppress selectively certain instabilities and hence check if it is their presence that leads to a certain level of turbulence.

In the course of this work we also developed a number of approximate methods that give the possibility to calculate easily the influence of certain parameters like ion-mass ratio, temperature ratio and light-ion concentration. It would be easy to extend the theory to include different temperatures and/or different charges for the two ion species.

## References

[1] A. J. D. Lambert, F. W. Sluijter and D. C. Schram, Physica 84C (1976) 394.
[2] E. A. Jackson, Phys. Fluids 3 (1960) 786.
[3] B. D. Fried and R. W. Gould, Phys. Fluids 4 (1961) 139.
[4] J. D. Jackson, J. Nucl. En. C 1 (1960) 171.